RADIATION DEFECTS AND RADIATION PROPERTIES OF METALS AND STRUCTURAL MATERIALS WITH DIFFERENT TYPES OF CRYSTAL LATTICES (EXPERIMENTS, MICROSTRUCTURES, MODELLING)

Viacheslav M. Chernov,

State Corporation for Atomic Energy "ROSATOM",
JSC "A.A. Bochvar High Technology Research Institute of Inorganic Materials" **(JSC "VNIINM")**, Moscow, Russia

- The main goals of theoretical, modelling and experimental investigations are to receive, compare and understand the mechanisms and the regularities of the formation of microstructure and functional properties of SMs under neutron irradiation and on this knowledge base to help the real materials science and technologies for further widening of temperature, mechanical and dose application windows of the advanced SMs for nuclear fission and fusion power reactors (mainly for their cores).

- Many functional properties (initial and irradiation) are general for all SMs. In such cases SMs as the solid states with some defects have a similar behavior of initial and irradiation properties (impurity segregations, strengthening, creep, fatigue, fracture) and to understand such properties it is enough to use the usual approximations (fa, the isotropic continuous theory). But some important irradiation properties of the SMs are very sensitive to the symmetry of crystal lattices (face centered cubical – FCC, body centered cubical – BCC, hexagonal close packed – HCP).

- The basic SMs for nuclear reactors have one of mentioned crystal lattices type (FCC, BCC, HCP). In these important cases it is necessary to use the anisotropic theory of the crystal lattices with the different types of the very specific anisotropic defects (0D-3D).

The symmetry of crystal lattice is necessary condition to realize the typical irradiation properties of SMs (steels and alloys) such as

(1) swelling (FCC),
(2) low temperature embrittlement (BCC),
(3) physical yield of a fatigue (BCC),
(4) growth (HCP),
and some others.

Why these specific initial and irradiation properties are realizing basically only for one type of the crystal lattices (BCC, FCC, HCP) is a very hard problem of the physical materials science, solid state physics and multi-scale modeling up to day. Generally speaking, today we do not understand why the different types of crystal lattices (BCC, FCC, HCP, etc) are formed. Empirical potentials or the first-principal methods and the models based on them are used to describe the well known experimental results only.

Really up to now there are no physical multi-scale models and ideas for such functional properties of SMs (steels and alloys) as mentioned above. The pointed out phenomena are absent or very weak in crystals with other symmetry type or in the isotropic models. The symmetry of crystal lattices and internal stresses in crystals with inner structure are the key questions, which must be included in all physical models of irradiation physical and mechanical properties of the real SMs.
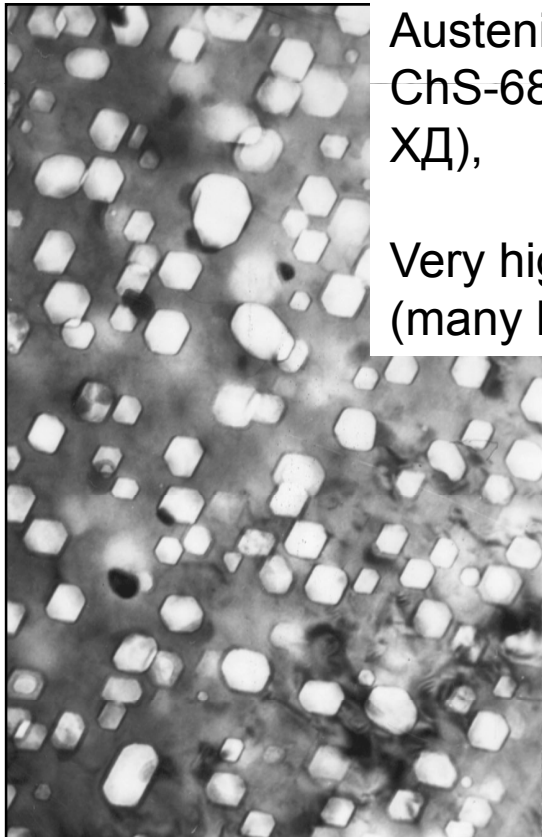
THE SMs CRITICAL PROPERTIES:

RADIATION SWELLING UNDER NEUTRON IRRADIATION – $(\Delta V/V)$max = 5-6 %

The unsolved problem for the FCC SMs (austenitic steels and alloys) and no optimism to fabricate the non(low)swelling austenitic steels (the FCC crystal lattice). We have no proofs - is it possible or impossible to fabricate the nonswelling austenitic (FCC) steel or alloy ?

Why ?

Q: How to fabricate the non(low)swelling SMs?
A: Use only the BCC Metals, fa, FMSs.

Austenitic SS (FCC): ChS-68 CW (ЧС 68 ХД),

Very high swelling (many big voids)

12%Cr FMS (BCC):

EP-450 (ЭП 450),

Very low swelling (seldom and small voids) up to dose 100 dpa

(d)   200 nm

4

THE SMs CRITICAL PROPERTIES:
LOW TEMPERATURE EMBITTLEMENT of the BCC metals
(ferritic-martensitic steels, vanadium alloys, etc.).
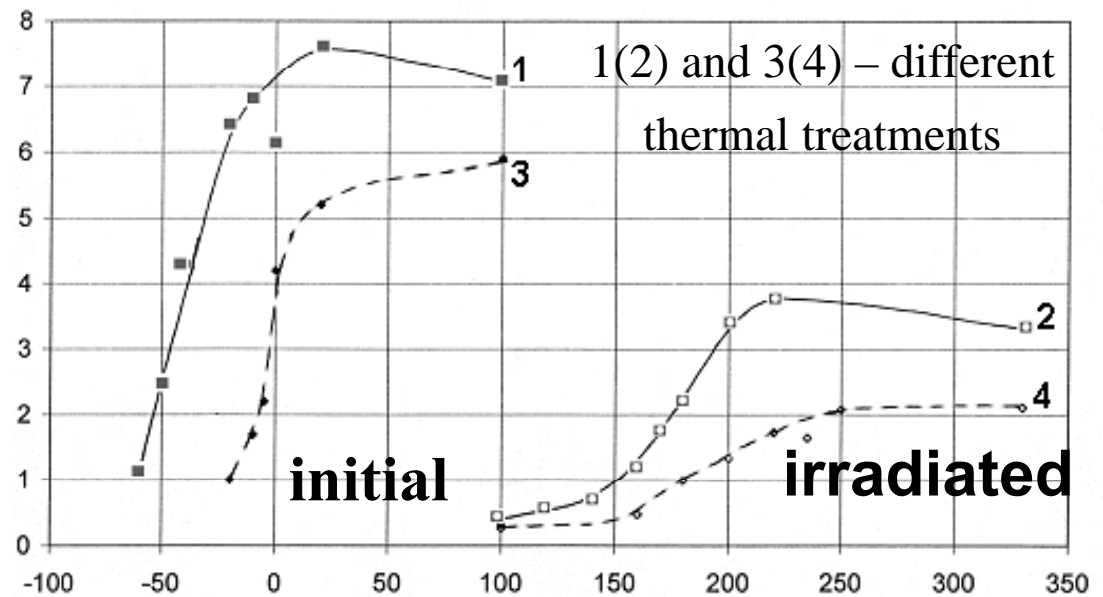
RAFMS Fe-12Cr-2W-V-Ta

The dependence of the DBTT from the specimen size (small and standard)
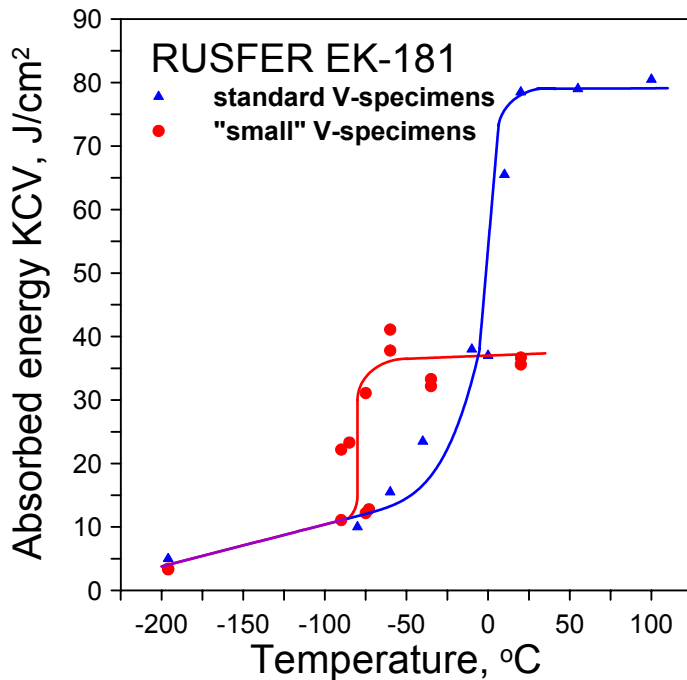
The shift of the DBTT under the low temperature (< 400 ^{0}C) irradiation

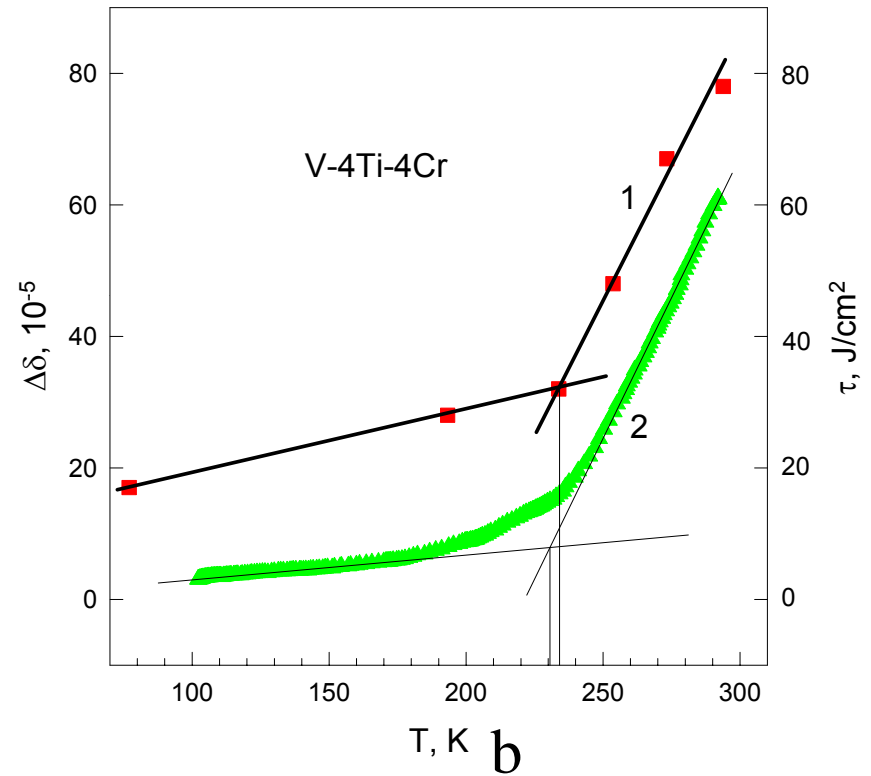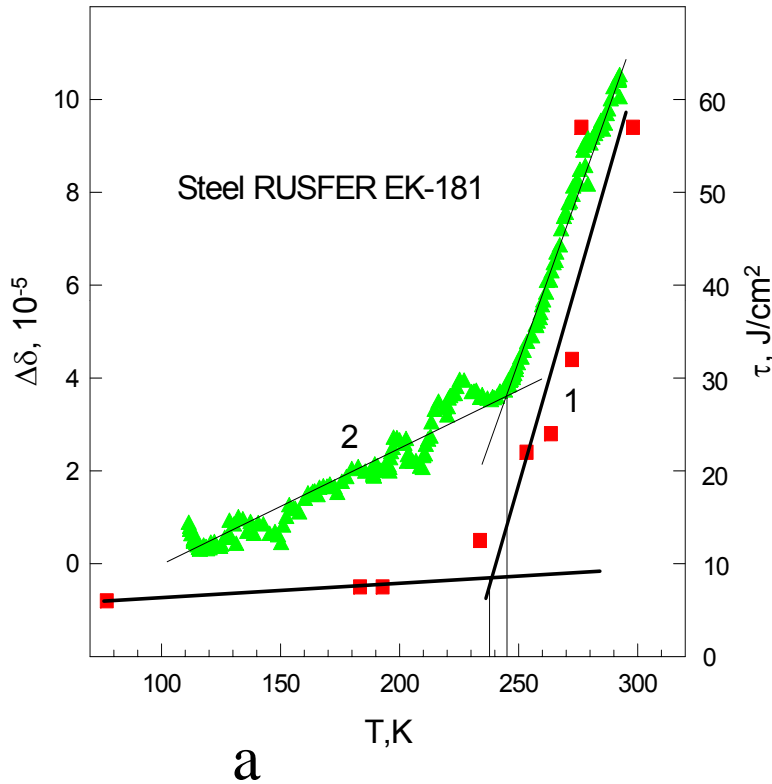**Fast reactor BOR-60, Tirr=340 ^{0}C, dose = 15 dpa.**

RUSFER EK-181
▲ standard V-specimens
● "small" V-specimens

1(2) and 3(4) – different thermal treatments

initial   irradiated

Q: How to fabricate the SMs without the LTIE ?

A: Use only the FCC metals (but swelling ?)

5

LOW TEMPERATURE EMBITTLEMENT AS PHYSICAL PROBLEM ?
RAFMS RUSFER-EK-181 / V-4Ti-4Cr (diamagnetics).

Temperature dependences of impact toughness (1) and logarithmic decrement (2)
for steel RAFMS RUSFER-EK-181 (a) and diamagnetic V-4Ti-4Cr alloy (b)

The DBTT in acoustic experiments (nondestructive test) are close in magnitude to the
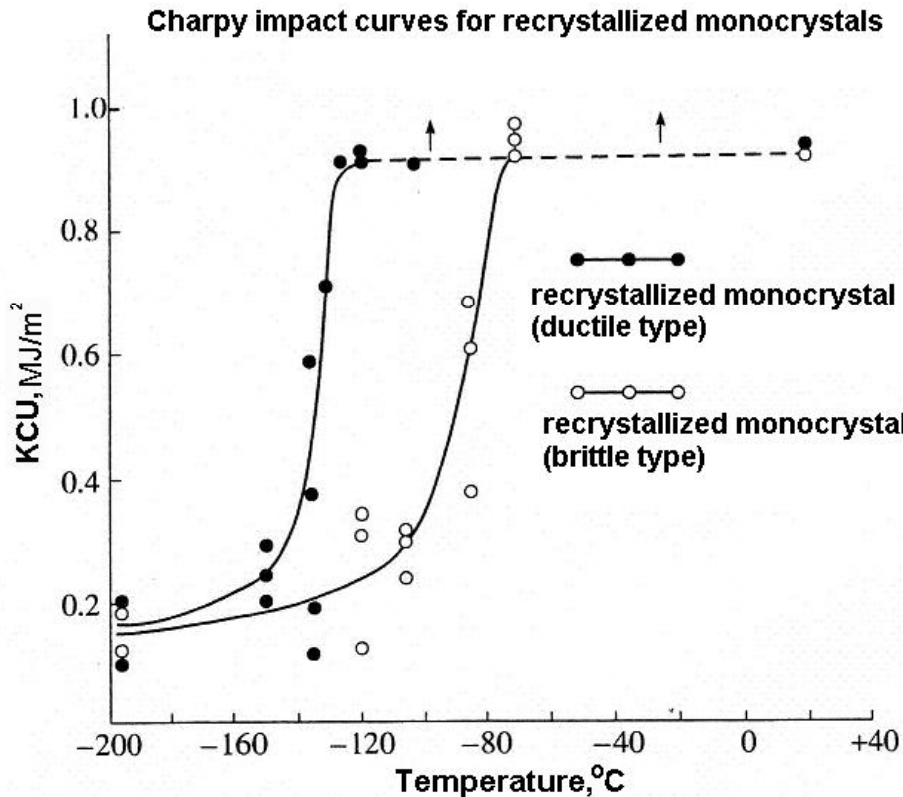DBTT measured by the destructive impact test (by chance or not by chance?).

FMS (the BCC): Impact Tests

PROBLEM OF THE LOW TEMPERATURE EMBRITLEMENT (LTE):
The influence of the grain boundaries ?
The RF Single Crystal FM Steels (plate and tubes)

Charpy impact curves for recrystallized monocrystals

recrystallized monocrystal (ductile type)

recrystallized monocrystal (brittle type)

The phenomenon of the LTE realizes in the BCC single crystals

7

The SMs CRITICAL PROPERTIES: THE FATIGUE OF METALS

Stress amplitude, σ_a

σ_a

σ_a

N_{G1} N_{G2}

Number of the stress cycles up to failure, N
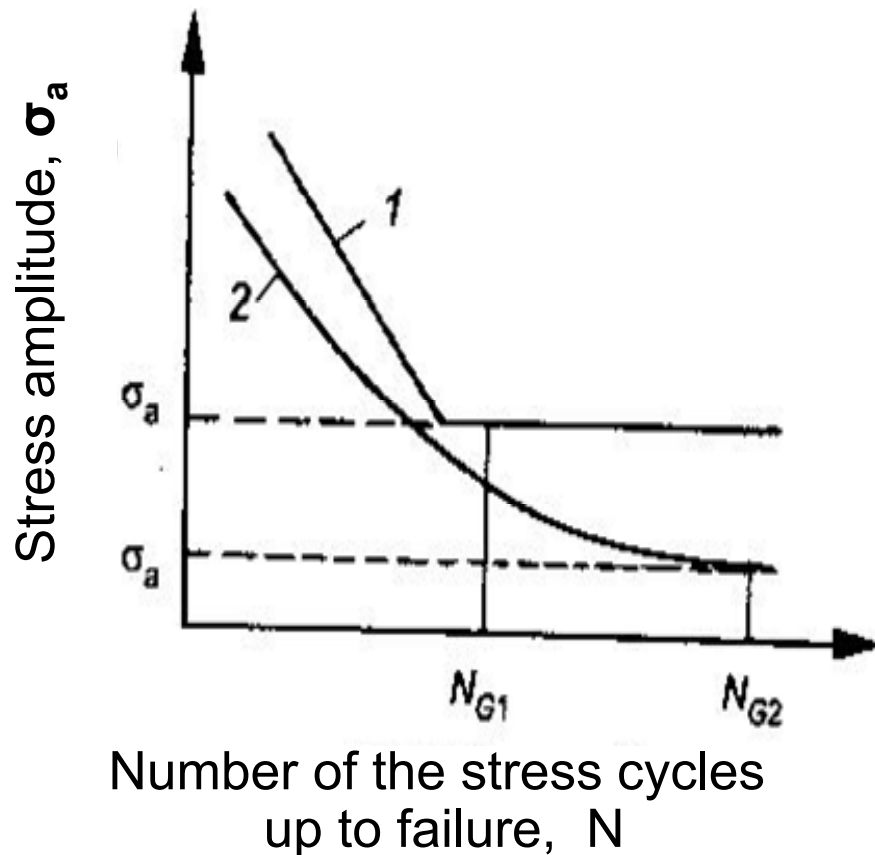
Typical fatigue curves for metals with the BCC (1) and the FCC (2) crystal lattices:

1. With the physical fatigue yield (typical curve for the BCC steels and alloys).

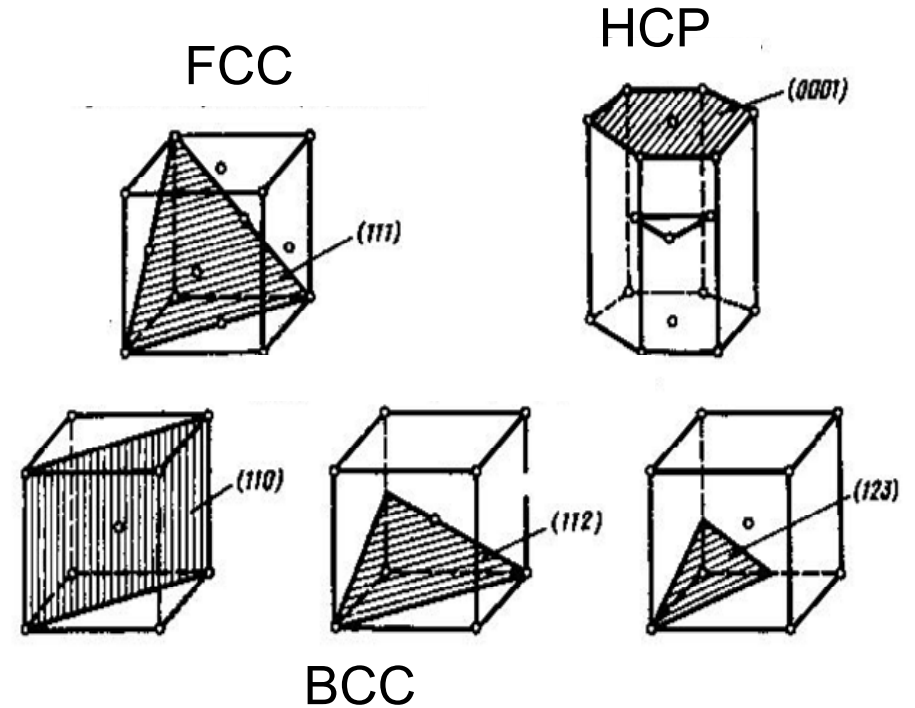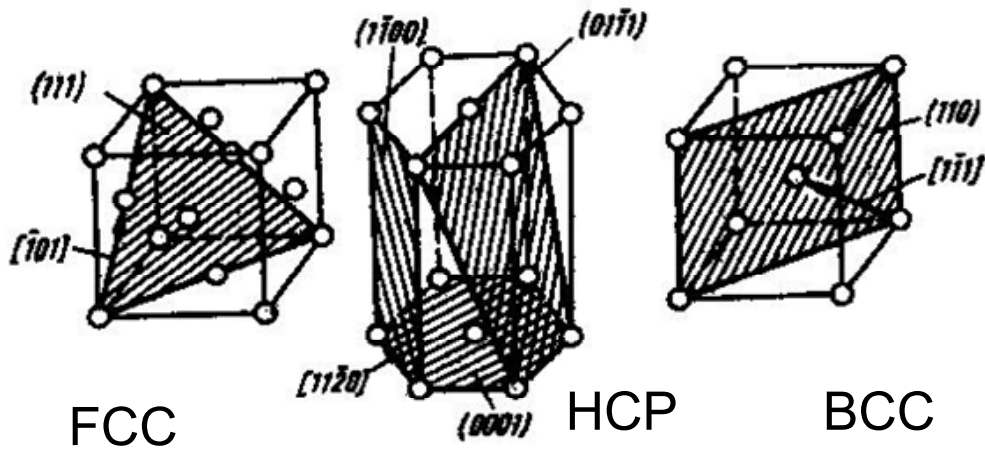2. Without the physical fatigue yield (typical curve for the FCC steels and alloys).

σ_a - critical parameters of the stress amplitudes.

N_{G1} and N_{G2} - critical numbers of the cycles

There are no satisfactory physical models for the fatigue behavior of the metals with different types of the crystal lattices

8

THE TYPICAL METALL CRYSTAL LATTICES

Planes (…) and Directions […] of closed packet crystals with the FCC, HP and BCC crystal lattices - the different glide systems (…)[…]

The glide planes of the FCC, HCP and BCC crystal lattices

Some types of dislocations
in crystal lattices with different symmetry

Lattice	Slip system	Burgers vector
BCC	<111>{110}	1/2<111>
	<111>{112}	1/2<111>
	<100>{001}	<100>
	<100>{110}	<100>
FCC	<110>{111}	1/2<110>
	<110>{110}	1/2<110>
HCP	$<11\bar{2}0>\{0001\}$	$1/3<11\bar{2}0>$
	$<0001>\{1\bar{1}00\}$	<0001>
	$<11\bar{2}3>\{1\bar{1}00\}$	$1/3<11\bar{2}3>$

ELASTIC ANISOTROPY OF CRYSTAL WITH THE DIFFERENT TYPES OF THE CRYSTAL LATTICES

C_{ij} – the elastic constants.

THE CYBIC CRYSTALS : $A = 2C_{44}/(C_{11}-C_{12})$, $N = C_{12}/(C_{11}+C_{12})$

(isotropic approximation $A = 1$. $N = \mathbf{v}$ – Poisson's coefficient).

For the FCC metals and alloys $A > 1$.

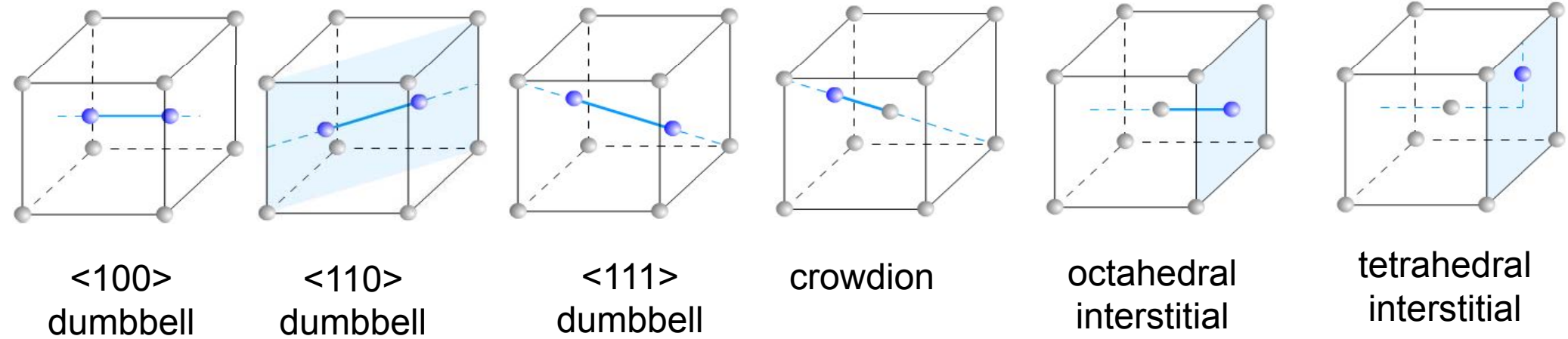For the BCC metals and Alloys $A > 1$ (Fe, Ta, others), $A = 1$ (W) and $A < 1$ (Cr, Mo, Nb, V, others).

THE HEXAGONAL CRYSTALS: $A = 2C_{44}/(C_{11}-C_{12})$, $B = C_{33}/C_{11}$, $C = C_{12}/C_{13}$
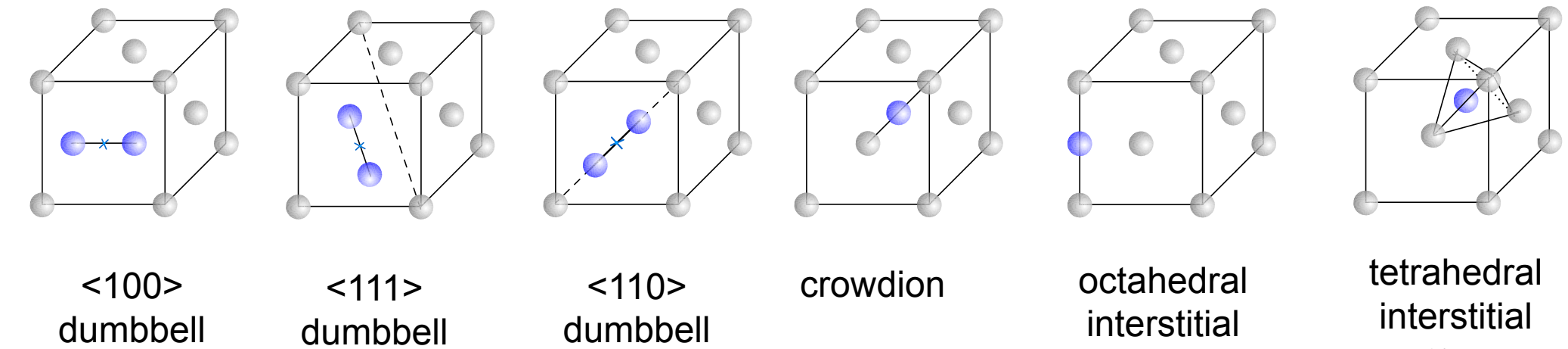(isotropic approximation A=B=C=1, no examples).

All anisotropic indexes (A, N. B. C) are depending from the temperature and the crystal anisotropy increases if the temperature increases.

The microstructures and functional properties of metal crystals are determined by the symmetry of crystals and their very specific defects: 0D (point defects, fa, vacancies, interstitial atoms), 1D (linear defects, fa, dislocations), 2D- surface defects, fa, grain boundaries, and 3D- volume defects, fa, phases.
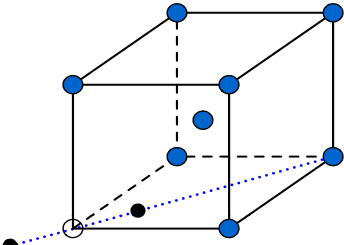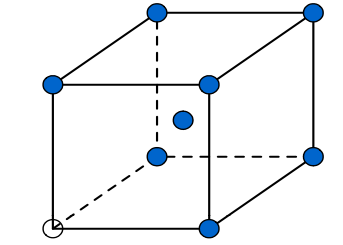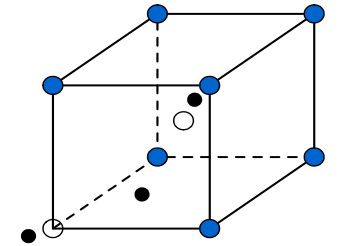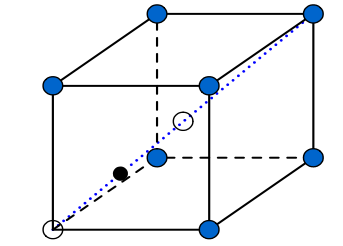
Self-point defect configurations in BCC lattice

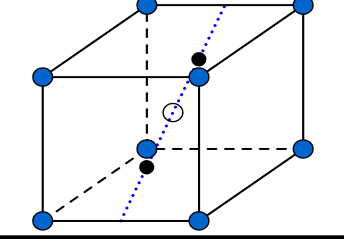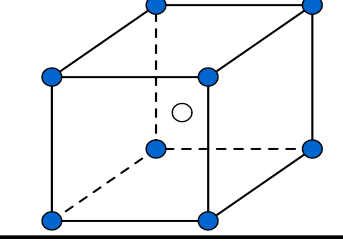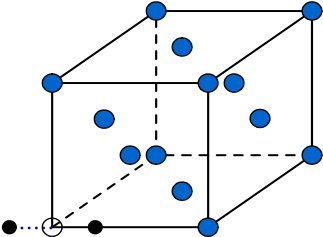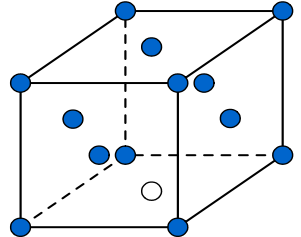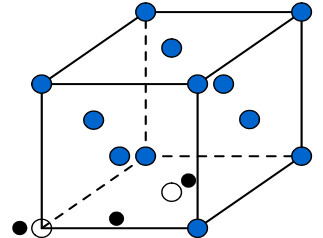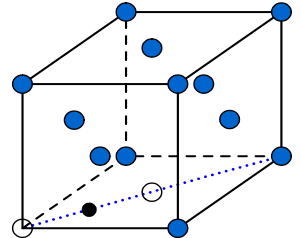| <100> dumbbell | <110> dumbbell | <111> dumbbell | crowdion | octahedral interstitial | tetrahedral interstitial |
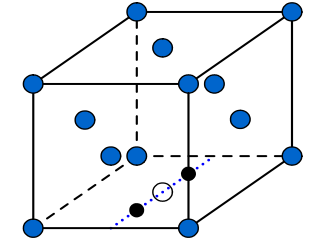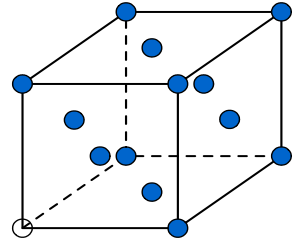
Self-point defect configurations in FCC lattice

| <100> dumbbell | <111> dumbbell | <110> dumbbell | crowdion | octahedral interstitial | tetrahedral interstitial |

Migration mechanisms of self-point defects (as elastic dipoles) in the BCC lattice

| $\langle 110 \rangle$ dumbbell	Symmetry and shape of P_{ij}	Vacancy	Symmetry and shape of P_{ij}
Stable	Orthorhombic $$\begin{pmatrix} P_{11} & P_{12} & 0 \\ P_{12} & P_{11} & 0 \\ 0 & 0 & P_{33} \end{pmatrix}$$	Stable	Cubic $$\begin{pmatrix} P_{11} & 0 & 0 \\ 0 & P_{11} & 0 \\ 0 & 0 & P_{11} \end{pmatrix}$$
Saddle point	Monoclinic $$\begin{pmatrix} P_{11} & P_{12} & P_{13} \\ P_{12} & P_{11} & P_{13} \\ P_{13} & P_{13} & P_{33} \end{pmatrix}$$	Saddle point	Trigonal $$\begin{pmatrix} P_{11} & P_{12} & P_{12} \\ P_{12} & P_{11} & P_{12} \\ P_{12} & P_{12} & P_{11} \end{pmatrix}$$
Stable	Orthorhombic $$\begin{pmatrix} P_{33} & 0 & 0 \\ 0 & P_{11} & P_{12} \\ 0 & P_{12} & P_{11} \end{pmatrix}$$	Stable	Cubic $$\begin{pmatrix} P_{11} & 0 & 0 \\ 0 & P_{11} & 0 \\ 0 & 0 & P_{11} \end{pmatrix}$$

Migration mechanisms of self-point defects (as elastic dipoles) in the FCC lattice

<100> dumbbell	Symmetry and shape of P_{ij}	Vacancy	Symmetry and shape of P_{ij}
Stable	Tetragonal $$\begin{pmatrix} P_{11} & 0 & 0 \\ 0 & P_{22} & 0 \\ 0 & 0 & P_{22} \end{pmatrix}$$	Stable	Cubic $$\begin{pmatrix} P_{11} & 0 & 0 \\ 0 & P_{11} & 0 \\ 0 & 0 & P_{11} \end{pmatrix}$$
Saddle point	Orthorhombic $$\begin{pmatrix} P_{11} & P_{12} & 0 \\ P_{12} & P_{11} & 0 \\ 0 & 0 & P_{33} \end{pmatrix}$$	Saddle point	Orthorhombic $$\begin{pmatrix} P_{11} & P_{12} & 0 \\ P_{12} & P_{11} & 0 \\ 0 & 0 & P_{33} \end{pmatrix}$$
Stable	Tetragonal $$\begin{pmatrix} P_{22} & 0 & 0 \\ 0 & P_{11} & 0 \\ 0 & 0 & P_{22} \end{pmatrix}$$	Stable	Cubic $$\begin{pmatrix} P_{11} & 0 & 0 \\ 0 & P_{11} & 0 \\ 0 & 0 & P_{11} \end{pmatrix}$$

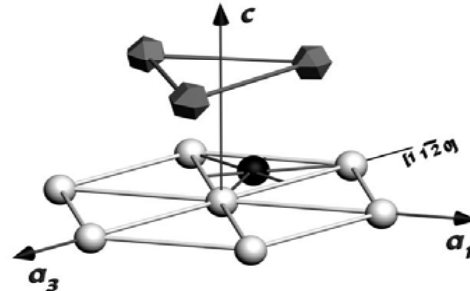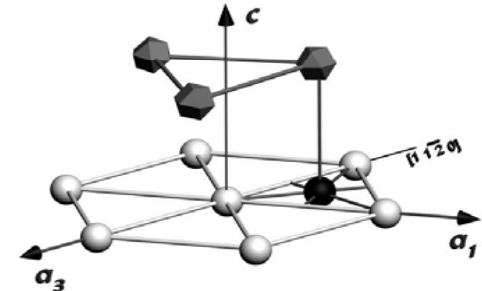# Self-point defect configurations in HCP lattice
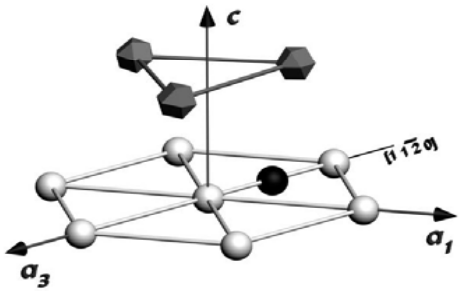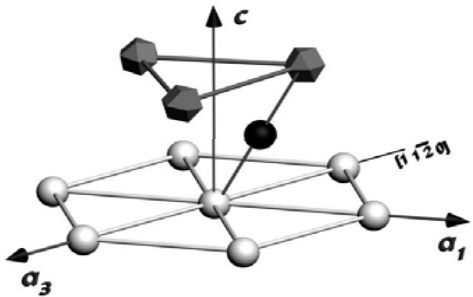

Basal crowdion
(BC)
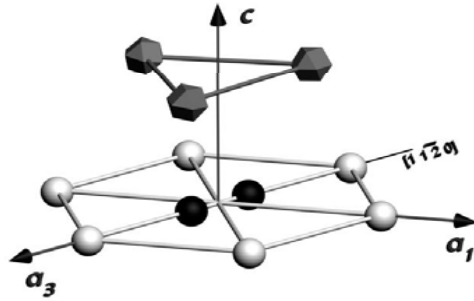
Basal split
interstitial (BS)

Basal octahedral
interstitial (BO)

Basal tetrahedral
interstitial (BO)

Crowdion
(C)
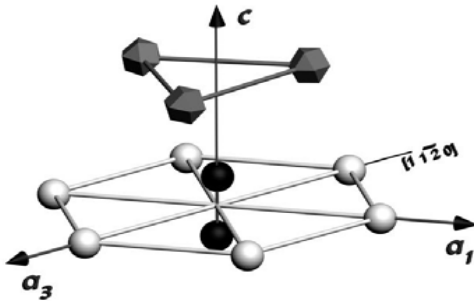
Split interstitial
(S)
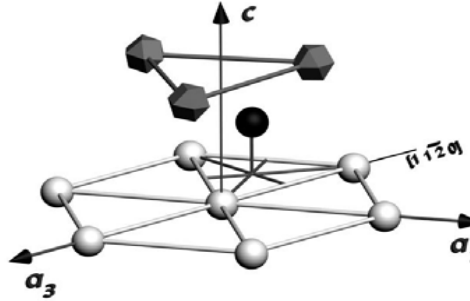
Octahedral
interstitial (O)
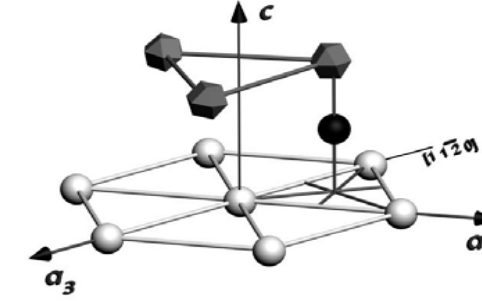
Tetrahedral
interstitial (T)

○ are the atoms of the basal plane $z = 0$

⬡ are the atoms of the basal plane $z = c/2$

● are the atoms composing SIA configuration

15

Migration mechanisms of self-point defects in HCP lattice

SIA migration mechanisms:

1) 1d migration: BC → BS → BC

2) BC migration in the basal plane with reorientation

3) BC migration out of a basal plane to the next basal plane

Vacancy migration mechanisms:

1) Vacancy migration in basal plane (jump direction <11-20>)

2) Vacancy migration out of a basal plane (jump direction <20-23>)
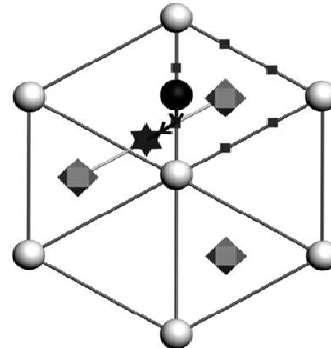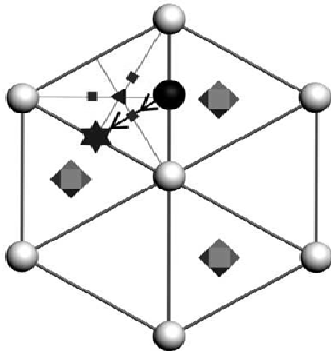
- ○ are the atoms of the basal plane $z = 0$
- ◆ are the atoms of the basal planes $z = \pm c/2$
- ▲ is BO configuration, $z = 0$
- ● is BC configuration before a jump, $z = 0$
- ★ is BC configuration after a jump
- ■ are the saddle points

16

Self-point defects characteristics in BCC Fe

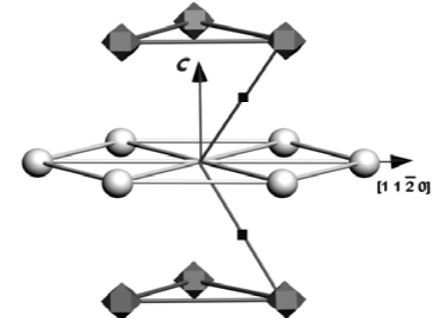| Defect configuration	E^F	V^R	P_{11}	P_{22}	P_{33}	P_{13}	P_{23}	P_{12}
<110> dumbbell	4.384	1.480	18.04	18.04	20.39	0	0	4.991
<110> dumbbell SP [a]	4.630	1.476	18.88	18.57	18.88	3.257	5.164	5.164
<111> dumbbell	4.627	1.436	18.27	18.27	18.27	6.365	6.365	6.365
Crowdion	4.635	1.442	18.35	18.35	18.35	6.322	6.322	6.322
Tetrahedral	5.149	1.286	15.60	16.74	16.74	0	0	0
Octahedral	5.464	1.174	21.02	11.89	11.89	0	0	0
<100> dumbbell	5.618	1.171	19.86	12.41	12.41	0	0	0
Vacancy	1.920	-0.140	-1.776	-1.776	-1.776	0	0	0
Vacancy SP	2.655	-0.112	-1.428	-1.428	-1.428	-1.684	-1.684	-1.684

E^F, P_{ij} in eV; V^R in atomic volumes

Self-point defects characteristics in BCC V

Defect configuration	E^F	V^R	P_{11}	P_{22}	P_{33}	P_{13}	P_{23}	P_{12}
<110> dumbbell	3.17	1.51	19.78	19.78	22.83	0	0	3.92
<110> dumbbell SP [a]	3.33	1.24	17.69	17.69	15.96	2.23	2.23	-0.59
<100> dumbbell	3.36	0.85	14.39	10.46	10.46	0	0	0
Octahedral	3.37	0.98	17.19	11.74	11.74	0	0	0
Tetrahedral	3.51	1.13	15.82	15.49	15.49	0	0	0
<111> dumbbell	3.58	1.25	17.25	17.25	17.25	4.48	4.48	4.48
Crowdion	3.60	1.26	17.42	17.42	17.42	4.56	4.56	4.56
Vacancy	2.79	-0.46	-6.36	-6.36	-6.36	0	0	0
Vacancy SP	3.21	-0.44	-6.11	-6.11	-6.11	-1.20	-1.20	-1.20

[a] SP – saddle point.

Sivak A.B., Chernov V.M., Dubasova N.A. et al. *J. Nucl. Mater.* **367-370** (2007) 316-321

Sivak A.B., Romanov V.A. and Chernov V.M *J. Nucl. Mater.* **323** (2003) 380-387

Self-point defects characteristics in FCC Cu

Self-point defect	E^F, eV	V^R, Ω	P_{11}, eV	P_{22}, eV	P_{33}, eV	P_{13}, eV	P_{23}, eV	P_{12}, eV
<100> dumbbell	3.068	1.848	18.55	18.99	18.99	0	0	0
<100> dumbbell saddle point	3.166	1.887	19.09	19.09	19.57	0	0	2.216
<110> dumbbell	3.302	1.906	18.38	18.38	21.57	0	0	10.48
Vacancy	1.272	-0.298	-3.044	-3.044	-3.044	0	0	0
Vacancy saddle point	1.962	-0.189	-3.720	-3.720	1.662	0	0	-0.7556

Self-point defects characteristics in HCP Zr

Self-point defect	E^F	V^R	$P^{(1)}$	$P^{(2)}$	$P^{(3)}$	$e^{(1)}$	$e^{(2)}$	$e^{(3)}$	N^*
BC	3.75	1.33	24.28	20.18	15.14	(1 0 0)	(0 1 0)	(0 0 1)	3
BS	3.77	1.35	24.47	20.38	15.48	(1 0 0)	(0 1 0)	(0 0 1)	3
C [1)]	3.98	1.28	13.80	17.77	26.44	(1 0 0)	(0 x y)	(0 -y x)	6
BO [**]	3.98	1.30	21.15	21.15	15.94	(1 0 0)	(0 1 0)	(0 0 1)	1
BT [**]	4.20	1.38	20.00	20.00	22.04	(1 0 0)	(0 1 0)	(0 0 1)	1
O [**]	4.13	1.50	19.00	19.00	30.10	(1 0 0)	(0 1 0)	(0 0 1)	1
T [**]	4.24	1.28	16.38	16.38	25.59	(1 0 0)	(0 1 0)	(0 0 1)	1
S	4.31	1.21	15.57	15.57	23.75	(1 0 0)	(0 1 0)	(0 0 1)	1
BC_{in}^{SP} [2)]	3.98	1.31	19.03	21.80	18.21	(1 0 0)	(0 x y)	(0 -y x)	6
BC_{out}^{SP} [3)]	3.98	1.38	18.74	17.63	25.95	(1 0 0)	(0 x y)	(0 -y x)	6
V	1.78	-0.27	-3.99	-3.99	-4.23	(1 0 0)	(0 1 0)	(0 0 1)	1
V_{in}^{SP}	2.62	-0.28	-9.08	-0.66	-2.81	(1 0 0)	(0 1 0)	(0 0 1)	3
V_{out}^{SP} [4)]	2.67	-0.32	-9.23	1.32	-6.66	(1 0 0)	(0 x y)	(0 -y x)	6

[*] $N = 1, 3, 6$ corresponds to trigonal, orthorhombic, monoclinic symmetries of elastic dipoles, respectively.

[**] Unstable configuration.

[1) - 4)] $y = \sqrt{1 - x^2}$; [1)] $x = 0.9965$; [2)] $x = 0.9403$; [3)] $x = 0.9989$; [4)] $x = 0.8710$.

SP is for saddle point.

Elastic interaction energy between SPDs (elastic dipoles P$_{ij}$) and dislocations

$$E_{\text{int}}(\mathbf{r}) = -P_{ij}\varepsilon_{ij}^{d}(\mathbf{r}) = E_0 \frac{b}{r} f(\phi), \quad \int_{0}^{2\pi} [f(\phi)]^2 \, d\phi = \pi$$

P_{ij} - the dipole tensor of the PD $\quad$ ε_{ij} - the elastic strain tensor

r - the defect radius vector $\quad\quad\quad$ **b** - the Burgers vector

ϕ - the angle between the abscissa axis and **r**

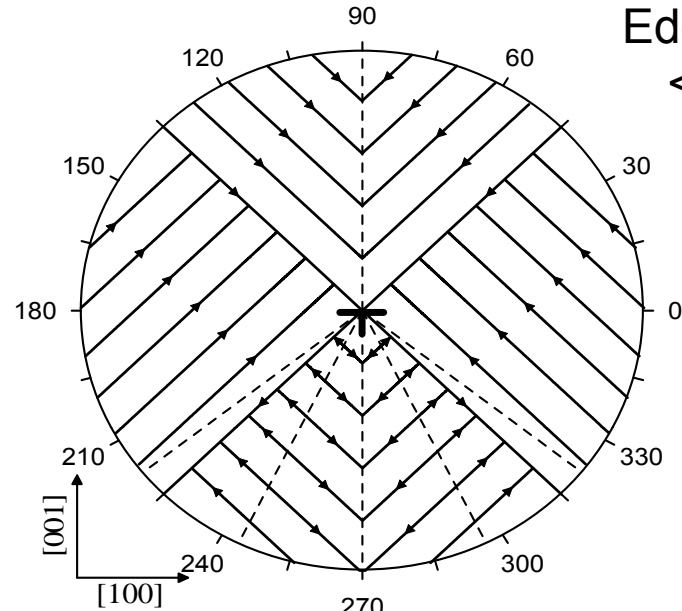## Influence of dislocation elastic fields on the migration directions of SPDs
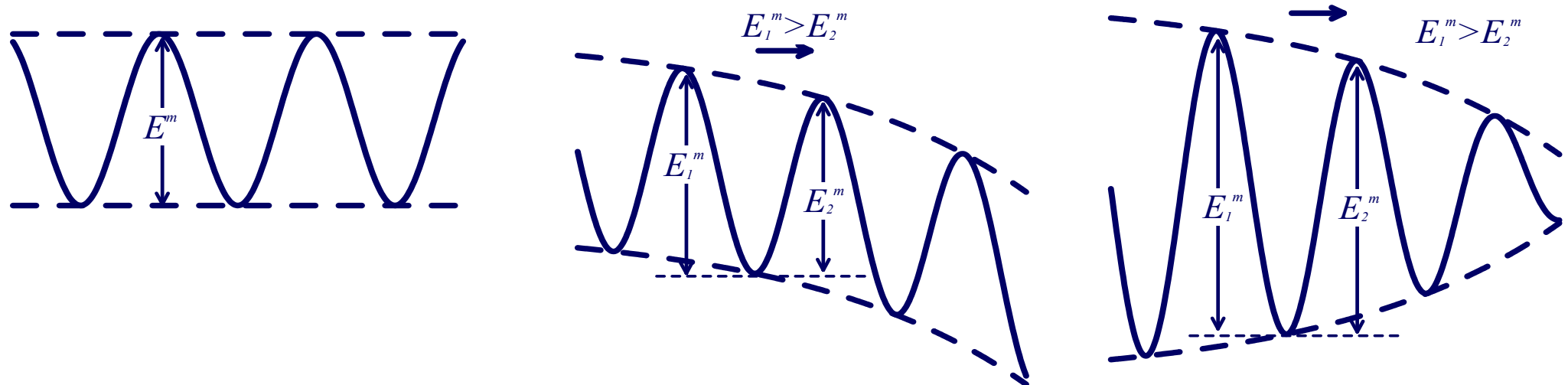
Energy barriers for SPD migration in case of absence of the dislocation stress fields (**a**) and in case of their presence (**b**, **c**)

Migration pathways of SIA with the lowest energy barriers in elastic fields of dislocations in BCC Fe
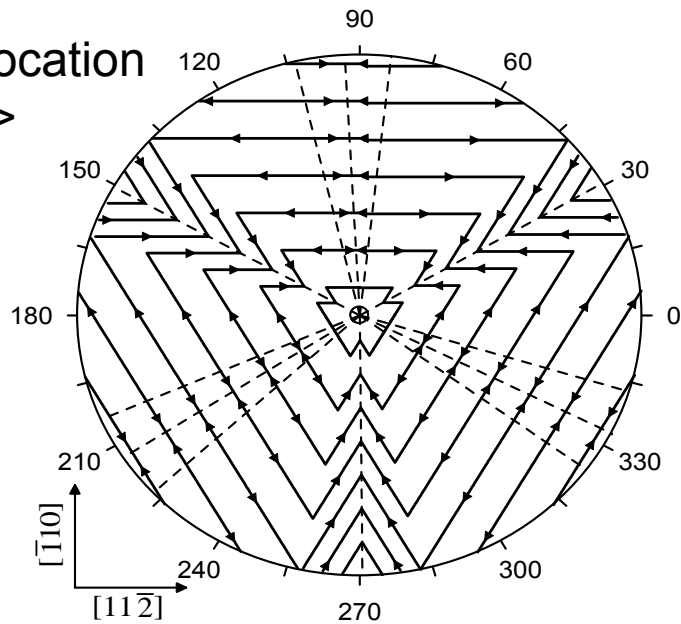
Edge dislocation
<111>{110}
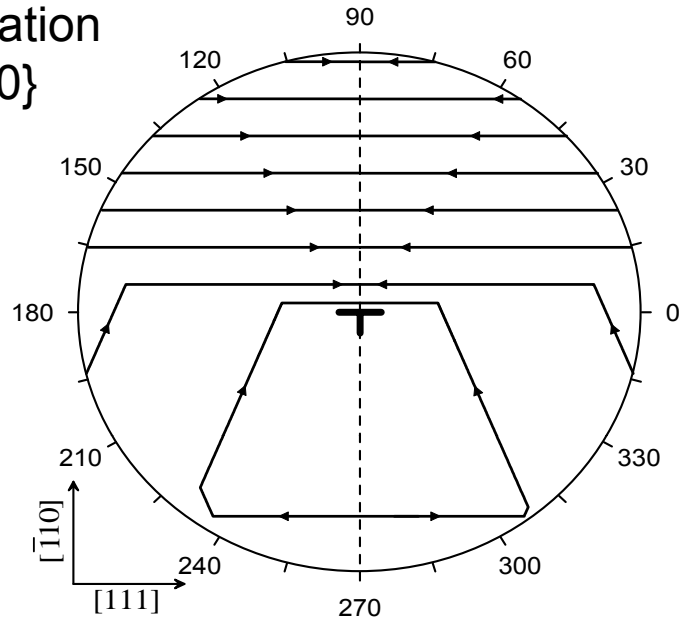
Edge dislocation
<100>{100}
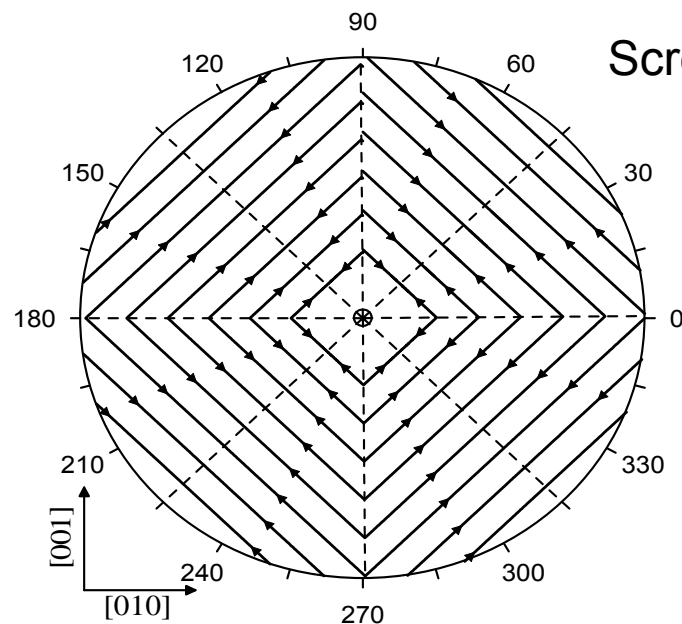
Screw dislocation
<111>

Screw dislocation
<100>

21

Migration pathways of SPDs with the lowest energy barriers in elastic fields of dislocations in FCC Cu
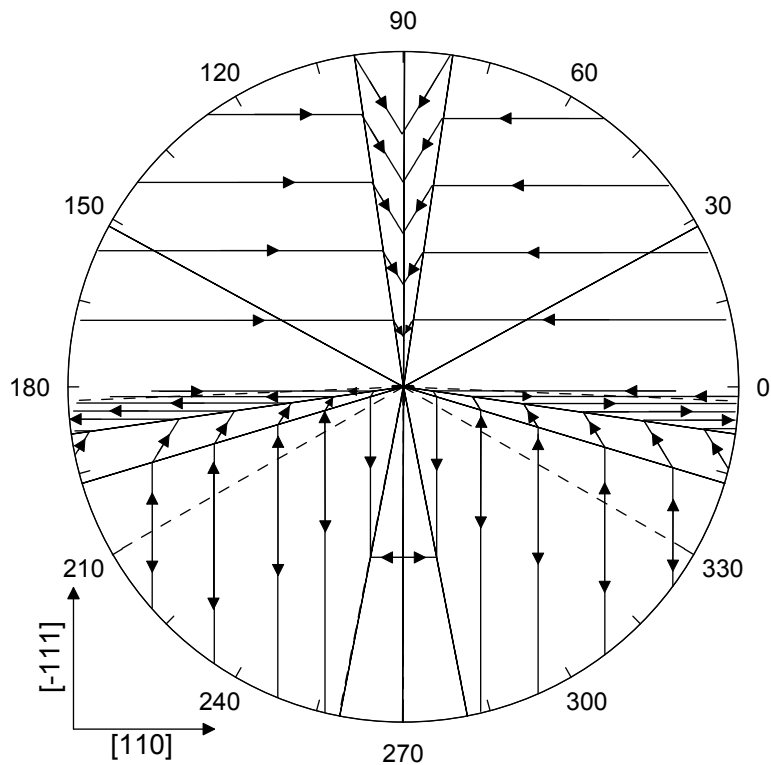
<110>{111} edge dislocation, <100> dumbbell
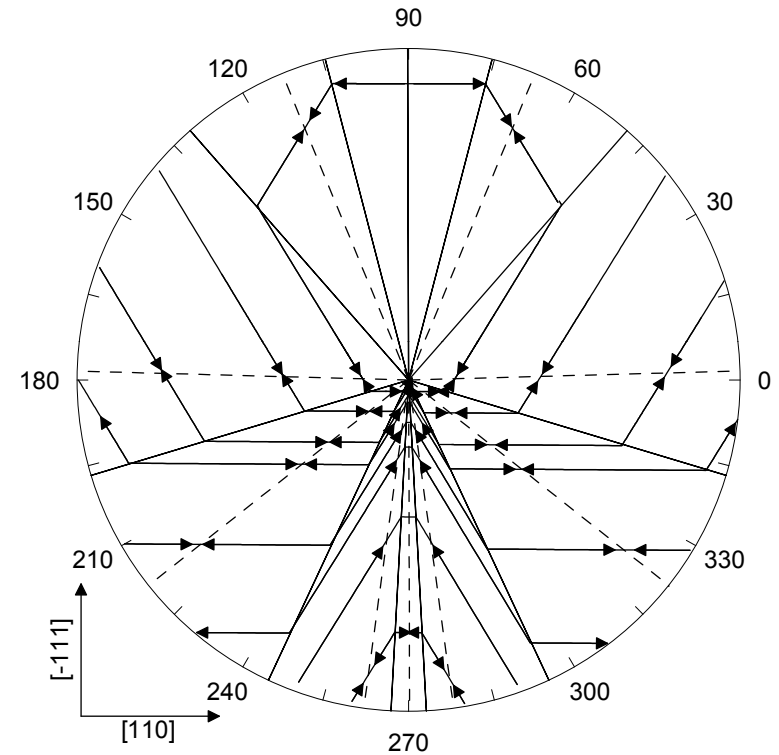
<110>{111} edge dislocation, vacancy

Migration energy of SPDs vs. distance to the edge dislocation <11-20>{0001} in HCP Zr
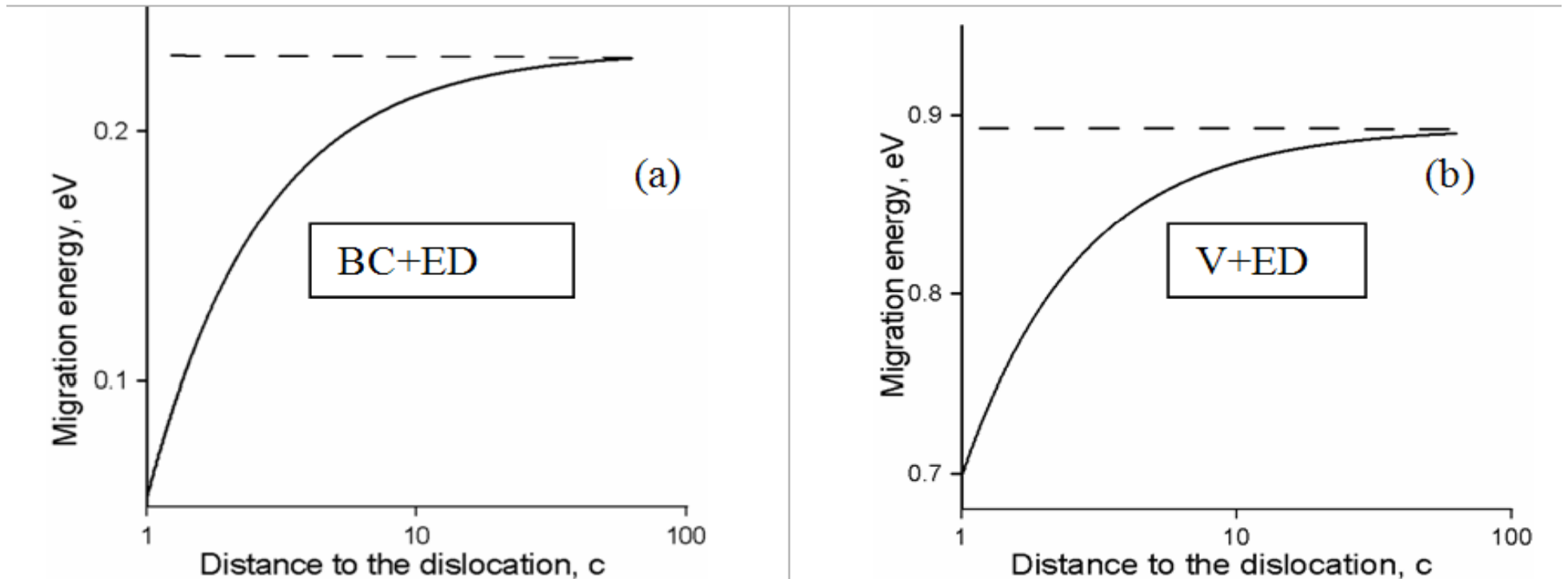
The solid line is the migration energy curve of an SPD heading to the edge dislocation. The dotted line is the migration energies in the absence of the dislocation: (a) SIA, (b) Vacancy

23

Dislocation sink strengths for SPDs in BCC iron

Kinetic Monte Carlo (kMC) simulation of SPD diffusion

Probability of SPD in "i" direction:

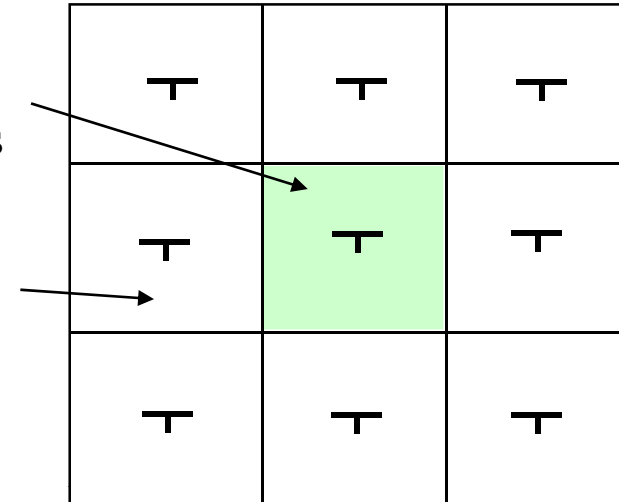$$p_i = \frac{\exp\left(-E_i^M \beta\right)}{\sum\limits_{i=1}^{n} \exp\left(-E_i^M \beta\right)} = \frac{\exp\left(-E_i^{\text{int}} \beta\right)}{\sum\limits_{i=1}^{n} \exp\left(-E_i^{\text{int}} \beta\right)}$$

E_i^M - SPD migration energy for "i" jump direction;

E_i^{int} - interaction energy between dislocation and SPD in corresponding saddle point configuration

Computational cell with periodic boundary conditions

Periodic images

Sink strength: $k^2 = 2d\big/\left(l^2 \langle N \rangle\right)$

d – dimensionality of diffusion ($d = 3$ in case of 3d diffusion);

l – jump length;

$<N>$ - average number of SPD jumps before absorption

Dislocation	k^2/ρ_d	
	SIA	Vacancy
<111>	3.75	2.23
<100>	4.50	2.82
<111>{110}	8.51	2.95
<100>{100}	8.54	2.65
without elastic field	2.11	2.11

Temperature 293 K

Dislocation density
$\rho_d = 3 \cdot 10^{14}$ m^{-2}

24

THE FCC.BCC and HCP crystals – the base characteristics (planes and directions of glide, point defects) and typical properties

(-) - no or very small, (+) – there are, (++) – as the typical phenomena

		FCC	BCC	HCP	
				1	2
Slip systems		{111}, {100} <110>	{110}, {112}, {123} <111>	{0001}, {1010}, {1011} <1120>, {1010} <0001>	{1011}, {2112} <2113>
Deformation by	glide	+	+	+	+
	twins	+	++	+	++
	creep	+	++	+	+
LTE / LTRE		–	++	–	+
Fatigue: Physical fatigue yield		+	++	+	++
Swelling		++	–(+)	+	–
Radiation growth		– (?)	–	+	++
Self point defects		<000>, <100>, <110>, <111> - elastic dipoles		trigonal, orthorombic, monoclinic and other elastic dipoles	
Impurity point defects					

Role of Simulations Based on Adequate Theory & Modeling

- Help to understanding of mechanisms and phenomena under temperature, stress and irradiation influences.

- Qualitative predictions of processes (fa, individual point defect properties in the stable and metastable positions, diffusion paths for the different stress states, etc.

- Quantitative predictions of properties
  - Processes on the micro-nano-mezo-macro- levels.
  - Macroscopic properties resulting from complex multiscale processes.
 - Model validation and calibration with experimental data is essential.

Role of Modeling and Experiment in Nuclear Power Development

- Can fusion power development go without fast power and other neutron sources?
  - No, only together with existing and future irradiation facilities (fa, IFMIF) and simulation.
  - No, licensing authority will not allow construction and operation without engineering data obtained by irradiation test data **in adequate conditions**.
- Can nuclear power development go without simulation?

  No. Since components of power fusion and fission reactors are exposed to very severe and complex environment, experimental data alone cannot cover all material conditions.
- Test matrix of the SMs properties will be optimized with the help of theory and modeling.
- Integrated research between physical theory & modeling & experiment will be the fastest way to realization of nuclear fusion and fission power.

Length scales of micro-/nanotomography techniques showing lateral versus depth resolution ranges for anisotropic or isotropic techniques.
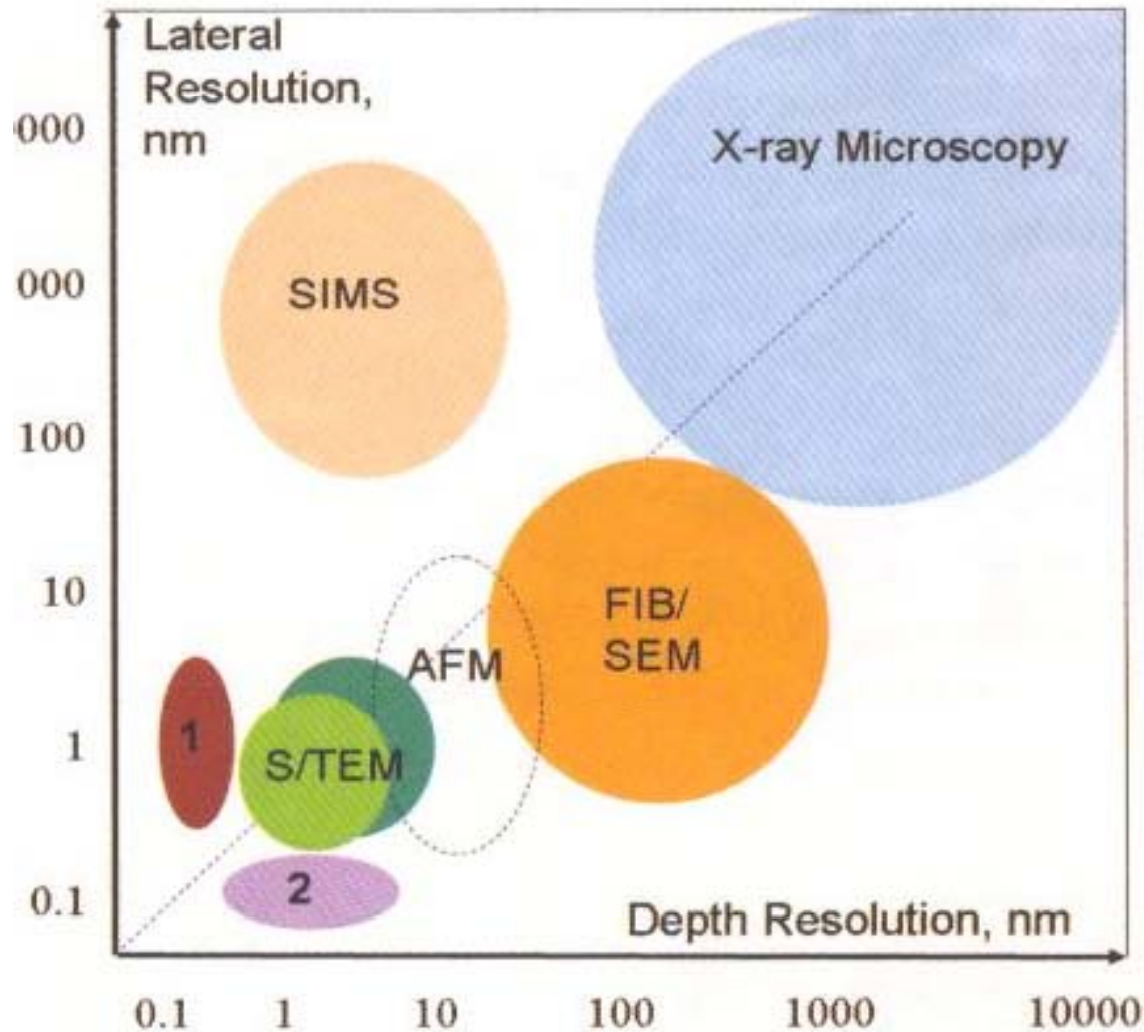
Green − Electron tomography.

1 = atom−probe tomography.

2 = scanning transmission electron microscopy (STEM) focal sectioning.

AFM = atomic force microscopy sectioning.

SIMS = secondary ion mass spectroscopy.

FIB/SEM = focused ion beam/scanning electron microscopy.

The observations of different dislocation and defect behavior that call our current understanding into question. The first observation of the diffusion of dislocations using in situ transmission electron microscopy (TEM).
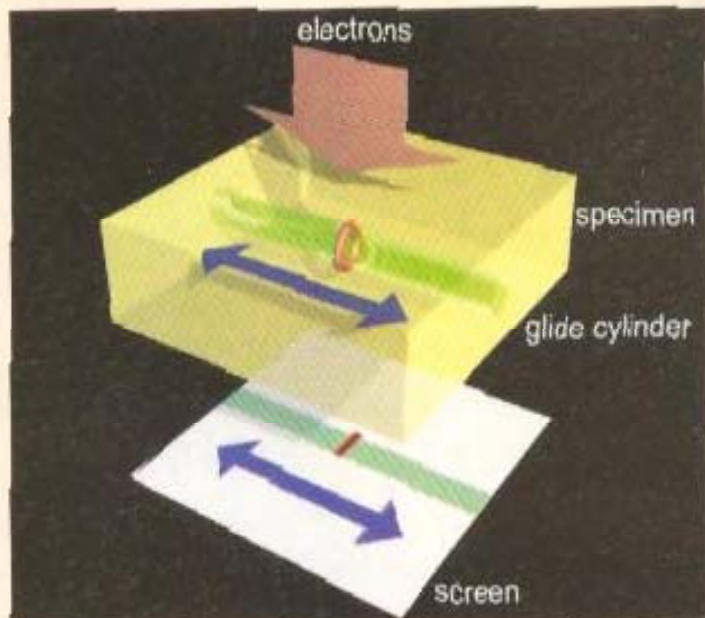
Schematic view of the observation of the one-dimensional glide motion of a nanometer-sized dislocation loop by TEM. The red ring is a dislocation loop. The direction of the motion of the loop is parallel to its Burgers vector. (© 2007 AAAS.)

2007. Kazuto Arakawa et all (Japan) have observed the nanometer-sized dislocation loops undergo one-dimensional diffusion in Fe (BCC) even in the absence of stress.

2007. Y. Matsukawa and S. Zinkle (USA) have observed the one-dimensional fast migration of nanometer-sized clusters of vacancies in FCC Au. The migration mode of vacancy clusters is different from that of single vacancies in Au. Vacancy-type dislocation loops exhibit one-dimension diffusion that is faster than single vacancies and comparable to SIAs.

The sizes of the dislocation loops that show the effect are significantly larger than expected from Molecular Dynamics Simulations.

CONCLUSION

THE NEW FUNDAMENTAL ASPECTS AND THE NEW SMs ARE REQUIRED FOR FUTHER WIDENING OF TEMPERATURE, MECHANICAL AND DOSE APPICATION WINDOWS TO REALIZE THE INNOVATIVE NUCLEAR POWER FUSION AND FISSION REACTORS IN THE FIRST HALF OF THE 21st CENTURE.

IT IS VERY NECESSARY THE NEW SCIENTIFIC AND TECHNOLOGY DECISIONS ("REVOLUTIONARY") FOR THE MATERIALS SCIENCE R&Ds ON THE BASE OF THE UNDERSTANDING THAT REAL SMs ARE THE MULTISCALE SINERGETIC OBJECTS INCLUDING THE MICRO-NANO-MEZO-MACRO-LEVELS WITH VERY SPECIFIC PROPERTIES OF THE MICRO-STRUCTURE AND PROPERTIES OF THE REAL ANISOTROPIC CRYSTALS WITH THE DIFFERENT TYPES OF THE CRYSTAL SYMMETRY.

THE NEW FUNDAMENTAL ASPECTS OF COMPUTATIONAL MATERIALS MODELLING ARE REQUIRED FOR THE QUANTITAVE ASSESMENT OF PROCESSES AND EVENTS NOT ACCESSIBLE TO DIRECT OBSERVATION.

"OUR NEAR FUTURE IS NUCLEAR FISSION & FUSION JOULE-POWER"

MY GRATITUDE TO THE IAEA & ICTP

Thanks for your Attention & Patience